Science and Technology Indonesia
e-ISSN:2580-4391 *p*-ISSN:2580-4405
Vol. 7, No. 4, October 2022

Research Paper

Study the Impact of Laser Energy on Laser-Induced Copper Plasma Parameters By Spectroscopic Analysis Technique

Ibrahim Karim Abbas[1]*

[1]*Department of Physics, College of Science, University of Baghdad, Baghdad, 10071, Iraq*
***Corresponding author:** Ibrahim.kareem1104a@sc.uobaghdad.edu.iq*

Abstract
In this paper, spectroscopic analysis (OES) for copper (Cu) plasma was achieved at atmospheric pressure. Q-switched Nd: YAG pulsed laser with a fundamental wavelength (1064 nm), energy range (500-800) mJ, frequency (6 Hz), and laser pulses (10-30 pulses) was applied to induce copper plasma. Based on the spectroscopic analysis, plasma parameters like electron temperature (T_e), electron density (n_e), Debye length (λ_D), and plasma frequency (f_p) have been calculated. The results demonstrated that the laser energy affects all plasma parameters, with an electron temperature (T_e) range of (0.6820-0.8949) eV and electron number density (n_e) range of (13.667-17.235)×10^{17} cm^{-3}. Also, the image of the place of laser bombardment of copper (Cu) metal shows three diameters or circles, each circle bears a different color from the other. It can be described as a crater, and the interaction of the laser with copper metal is obvious by laser ablation, and here the effect of the increased energy of the laser appears during the spectroscopic diagnosis and the process of metal bombardment.

Keywords
Copper Plasma, Electron Temperature, Laser-Induced Plasma, Plasma Parameter, Optical Emission Spectroscopic (OES)

Received: 26 July 2022, Accepted: 15 October 2022
https://doi.org/10.26554/sti.2022.7.4.508-513

1. INTRODUCTION

Laser Induced Breakdown Spectroscopy (LIBS) (Garcimuno et al., 2013), is a type of atomic emission spectroscopy that uses high-energy laser pulses as the driving force behind the excitation of optical materials (Fikry et al., 2020b). In certain communities, individuals also refer to it as laser-induced plasma spectroscopy (LIPS). The plasma that is produced as a result of the contact of high-intensity laser pulses with metal surfaces may be used, as is well knowledge, to generate very pure metal spectral lines (Caneve et al., 2006; Maurya et al., 2020). This can be accomplished by using the plasma created as a result of the interaction (Chaudhary et al., 2016).

In a nutshell, the laser pulse has a high intensity and is targeted on a small area of the sample surface in order to cause excitation of the optical sample, which is then evaluated (Yuan et al., 2020). This is done in to assess the sample's optical properties (Alberti et al., 2019). After that, procedures such as heating, evaporation, atomization, and ionization are carried out on a relatively small quantity of the material (Singh and Thakur, 2020). Following these processes will result in the generation of laser-induced plasma, often known as LIP (Pathak et al., 2012; Singh and Thakur, 2020).

LIP is an ionized substance that provides a source of metal spectra that are exceptionally free of impurities (Fernandes Andrade et al., 2021). After being brought back down to room temperature, the sample is remelted in the subsequent phase (Chaudhary et al., 2016). Wang et al. (2021b) focused on the importance of the electron-ion recombination and free-free interaction in plasma optical emissions (OES) produce spectral lines that are typical of the constituent species. (Chaudhary et al., 2016; Radziemski, 2020) In plasma processing and technology, as well as in fundamental scientific fields such as astrophysics and plasma physics, plasma spectroscopy is a crucial diagnostic approach; therefore, this research focuses on metals diagnostic, such as copper. Alberti et al. (2019) indicate the temperature of a plasma may be used to divide it into two primary categories, known as the high-temperature or fusion plasma and the low-temperature or gas discharge plasma, which focuses on the measurement of the electron temperature (OES) in laser-induced plasms. These are the classifications that are most helpful for describing plasmas by characteristics of plasma, including wavelength, energy, and pulse duration, which are considered essential (Shah et al., 2020).

Simultaneously, the level of plasma emissions are affected by the constituents of the surrounding atmosphere, as well as other factors that include temperature, pressure, and electric

field (Fikry et al., 2020a). In addition, the physical and chemical characteristics of the sample are considered important in this process (Wang et al., 2021a; Radziemski, 2020). In general, plasma has three essential properties, which are temperature, density, and quantity of emissions (Benedikt et al., 2021).

It is abundantly obvious that Nd:YAG has the capability of detecting copper spectrum (Akhtar et al., 2019). On the other hand, with the LIBS approach, as shown in the Figure 1, the pressure that was maintained around the sample was identical to that of the surrounding atmosphere (Singh and Thakur, 2020). This work aims to apply the spectroscopic analysis of the plasma produced from the copper element after the laser ablation by the Nd: YAG laser, where the resulting emission spectral lines are studied and the plasma parameters of the copper element are measured at different laser energies, including the electron temperature and the electron density in the produced plasma.

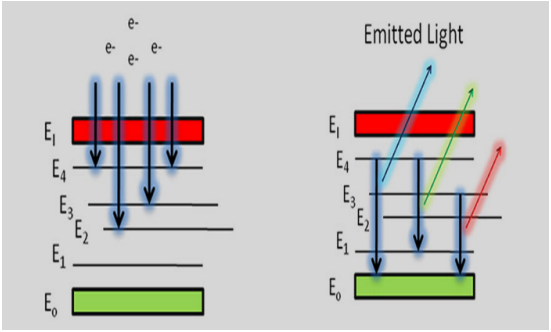

Figure 1. A Metal Surface is Laser-Ablated, and Light is Emitted in Continuous Lines as Plasma is Formed (Singh and Thakur, 2020)

2. EXPERIMENTAL SECTION

2.1 Preparation of Copper Plate to Laser Bombing Process

In the current experiment, the copper plate (Cu) sample has a purity is 99.99% obtained from E. Merck company, a diameter of 1 cm^2, and a thickness of 0.8 mm is square-shaped. (Cu) sample plate was placed under the laser lens and prepared for the laser bombing process.

2.2 Setup of Spectroscopic and LIBS System

Nd-YAG laser was used at a fundamental wavelength of 1064 nm and laser energy ranging from (500-800) mJ and a frequency of 6 Hz. An experiment was achieved at atmospheric pressure. The copper plate was positioned 10 cm away from the laser head to expose it to the bombardment process that would be carried out by various laser pulses (10-30 pulses). The purpose of carrying out these procedures was to achieve the objective of collecting the optical plasma emissions of the spectrum emitted by the copper sample via the spectrometer instrument's optical cable.

The angle at which the plasma emissions were captured by the spectrometer was 45°, and the distance between it and the copper plate was quite close-approximately one cm as shown in Figure 2 and accordingly, spectrum data were collected for each laser energy in a period not later than (30 sec), there was no delay after each laser energy. However, once the data is collected for this energy, directly transfers to collect data of laser energy that follows, and so on. The gate width of the OES diagnostic for the purpose of collecting data for the spectrum is 10 ns. The database provided by the National Institute of Standards and Technology (NIST), this database gives access and search capability for critically evaluated data on atomic energy levels, wavelengths, and transition probabilities in spectrum lines. In addition to this, the parameters of the laser-induced copper plasma were determined by utilizing spectroscopic data.

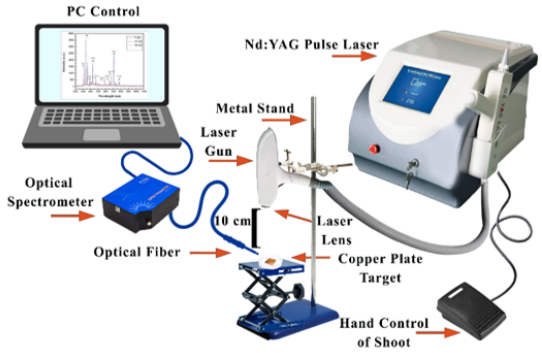

Figure 2. Configuration Setup of Spectroscopic Device and LIBS System for Diagnosing Copper Plasma Spectral

3. RESULT AND DISCUSSION

The image taken of the place of laser bombardment of copper metal shows three diameters or circles, each circle bears a different color from the other. As it appears in Figure 3: The outer diameter of the large circle is black, while the second diameter of the circle is as close to gray as possible, while the small central inner diameter of the place of bombing is close to brown. It is subjected to the strongest heating by the laser, as the image can be described as a crater and the interaction of the laser with copper metal is obvious, and the reason for this is that laser ablation is thermal, as the recoil pressure generated from the surface of the metal during its interaction with the laser beam causes the formation of a radial structure corresponding to the ejection of the dissolved material from the central region of the place of bombardment due to the expanding plasma, and here the effect of the increased energy of the laser appears during the spectroscopic diagnosis and the process of metal bombardment (Fikry et al., 2020b).

Figure 4 depicts the emission spectrum of copper metal plasma that was diagnosed by (S3000-UV-NIR) spectrometer at different laser energy, ranging from 500 to 800 mJ, where the figure shows that the spectrum was recorded from wavelengths ranging from 200 nm to 650 nm, where the results showed the emergence of many spectral copper peaks of these emissions, including several spectral lines for the atomic copper

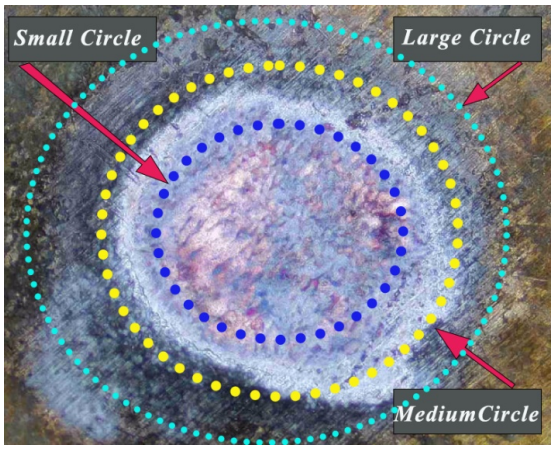

Figure 3. Magnification Image of Laser Bombardment Place in Copper Metal at 1064 nm for Different Laser Energies (500-800) mJ

Cu(I), which begin from the weak intensity 311.83 nm and 324.58, 346.62, 360.20 to the strongest intensity 521.32 nm, in addition, there were five ionic emission lines in the spectrum emissions lines Cu(II) starting from weak line 212.54 nm and 219.60, 237.82, 261.97 to the strongest line at 529.42 nm of the laser energy utilized (500-800) mJ. In situations where the intensity of these emission spectral peaks rises as a result of an increase in laser energy as a result of an increase in plasma absorption, copper emission spectral lines are the most useful for estimating plasma temperature, and thus plasma temperature estimations are greatly affected by resonant emission spectral lines, and agreement with prior findings (Ahmed and Yousef, 2021; Fikry et al., 2020a; Safeen et al., 2019).

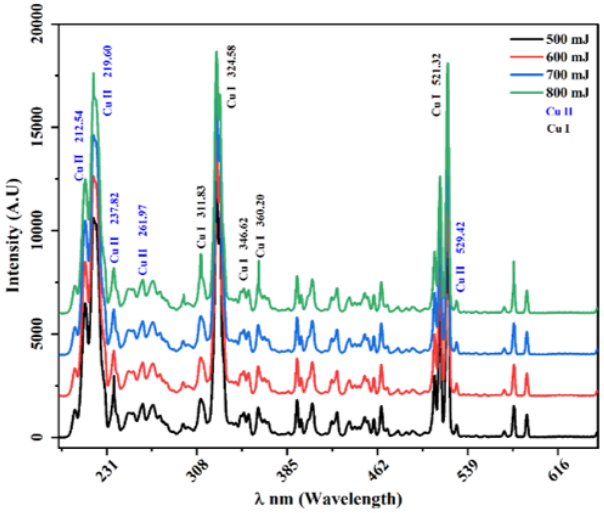

Figure 4. The Emission Spectrum of Copper Metal Plasma by LIBS Technique at (200–650) nm Generated by 1064 nm for Different Laser Energies (500-800) mJ

Plasma temperature has long been recognized as one of the most important characteristics in plasma physics, with also plasma parameters (Haberberger et al., 2019). To fully comprehend other plasma features, such as energy concentrations and particle velocities, it is necessary to know the plasma temperature. To determine the electron temperature values, the Boltzmann method was used, which is a common and widely used method to decide the spectroscopic parameters as in Equation (1) (Akatsuka, 2019).

$$\ln\left[\frac{\lambda_{ji} I_{ji}}{hcA_{ji}g_{ji}}\right] = -\frac{1}{KT}(E_j) + \ln\left|\frac{N}{U(T)}\right| \quad (1)$$

where g: statistical weight, λ: wavelength, E excited-state energy in eV, I_{ji}: intensity, A_{ji}: transition probability, N: densities of the state's total population and K: Boltzmann constant. So, the electron density can be given by the following formula and introduced as Equation (2) (Akatsuka, 2019):

$$n_e = \left[\frac{\Delta\lambda}{2\omega_s}\right] N_r(\mathrm{cm}^{-3}) \quad (2)$$

where $\Delta\lambda$ is the FWHM nm of the line, and ωs is the Stark broadening parameter that can be found in the standard tables, Nr is the reference electron density. On the other hand, it is known, that the laser-induced plasma information about the electron temperature and electron number density is critical due to clarifying the process of plasma production through laser bombardment, as well as LIBS, which are improved through the process of atomization, dissociation, and excitation at various-laser energies (Alberti et al., 2019). The frequency of plasma is determined from the following Equation (3) (Benedikt et al., 2021):

$$f_p = 8.98\sqrt{n_e}(\mathrm{Hz}) \quad (3)$$

One of the most fundamental features of plasma is its frequency (f_p), which is solely dependent on density. Because electrons have such a small mass, plasma has a high frequency. Debye shielding λ_D is a charged particle response that reduces the impact of electricity on local fields, giving the plasma its quasi-neutrality. To refer to the length of Debye λ_D, we can use the abbreviation λ_D and calculate from Equation (4) (Wu et al., 2021):

$$\lambda_D = \sqrt{\frac{\varepsilon_0 K_B T_e}{n_e e^2}} = 743 \times \sqrt{\frac{T_e}{n_e}} \quad (4)$$

Figure 5 illustrates the values of electron temperature in eV and Kelvin, the proportional rise with laser energy (500-800) mJ. The values start at 0.682 eV when the laser energy is 500 mJ and reach 0.894 eV when the laser energy is 800 mJ. Therefore, the findings revealed that the electron temperature, as well as the electron number density, rose with the increased energy of

the focused laser on a copper plate, with values corresponding to energies ranging from (13.667-17.235)×10^{17} cm^{-3}. As a consequence of this, the frequency of the plasma has a direct connection to and is proportionate to the electron density. As a result, we see what appears to be an increase in the frequency of the plasma, which is produced by an increase in the number of collisions that take place at high energies.

These subsequent equations represent the most important basic properties through which to describe the plasma generated from the laser bombardment process in metal, where Tables 1 indicated measured values of electron temperature (T_e), electron density (n_e), Debye length (λ_D), and plasma frequency (f_p), where plasma parameters measured using Boltzmann's theory of spectral lines of atom or ion of same ionization stage (Akatsuka, 2019).

Figure 5 illustrates the values of electron temperature in eV and Kelvin, the proportional rise with laser energy (500-800) mJ. The values start at 0.682 eV when the laser energy is 500 mJ and reach 0.894 eV when the laser energy is 800 mJ. Therefore, the findings revealed that the electron temperature, as well as the electron number density, rose with the increased energy of the focused laser on a copper plate, with values corresponding to energies ranging from (13.667-17.235)×10^{17} cm^{-3}. As a consequence of this, the frequency of the plasma has a direct connection to and is proportionate to the electron density. As a result, we see what appears to be an increase in the frequency of the plasma, which is produced by an increase in the number of collisions that take place at high energies.

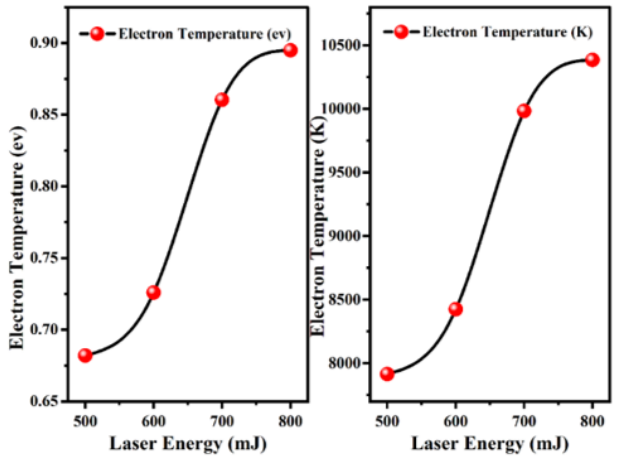

Figure 5. Variation Values of Electron Temperature and Proportional Increased with Laser Energy (500-800) mJ

It has been noticed that the temperature of the electrons at the surface of the target is higher than the temperature at the front end of the system. This occurs as a result of the continual absorption of radiation that takes place during the interaction of a laser pulse with an electron through the inverse bremsstrahlung absorption process (Kurniawan et al., 2018). So the energy of the laser is raised, a greater number of ions and free electrons are generated. The observed stark broadened line profile of an isolated line of either neutral atom or single charge ion is one of the most dependable ways for determining the electron number density. The electron number density (n_e) of the Stark broadening lines in relation to their full width at half maximum (FWHM) is shown in Figure 6. Consequently, through the values data obtained for the highest peaks for the copper plate target and when represented and plotted ln ($\lambda_{ji} I_{ji}/hcA_{ji}g_{ji}$) with E_j, we can calculate the electron temperature from the slope of the linear fitting of the resulting curve in Figure 8 and using Equation (1); in addition, it is also indispensable to determine the electron density and calculate it through Equation (2) as in Figure 7.

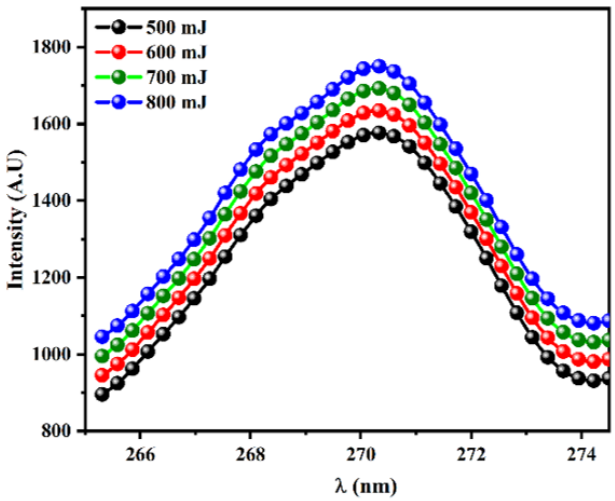

Figure 6. Full Width at Half Maximum (FWHM) to Laser Energy at (500-800) mJ for Wavelength Range (265.5-274) nm

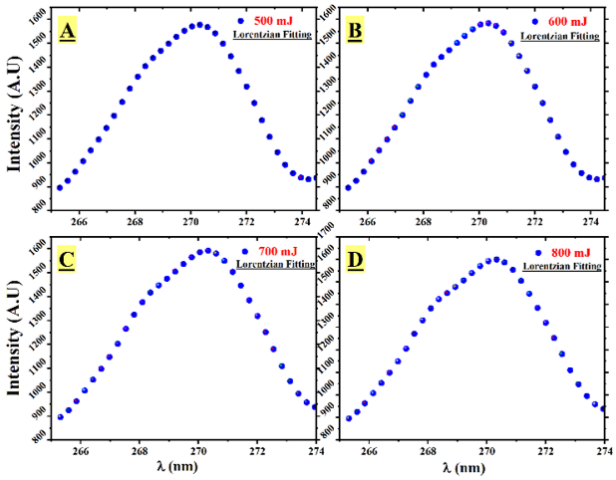

Figure 7. The Relationship Between Intensity and Wavelength (nm) at The Highest Peak Intensity for Different Laser Energy Values (500-800) mJ

Table 1. Laser-Induced Plasma Parameters for Copper Metal at Different Laser Energy (500-800) mJ

E (mJ)	λ_D (cm)	f_p (Hz)	n_e (cm^{-3})	FWHM (nm)	T_e (K)	T_e (eV)
500	0.524×10^{-6}	10.498×10^{12}	13.667×10^{17}	4.000	7914.75	0.6820
600	0.532×10^{-6}	10.826×10^{12}	14.534×10^{17}	4.500	8423.95	0.7259
700	0.575×10^{-6}	11.644×10^{12}	16.814×10^{17}	5.100	998383	0.8603
800	0.563×10^{-6}	11.789×10^{12}	17.235×10^{17}	5.200	10,385.01	0.8949

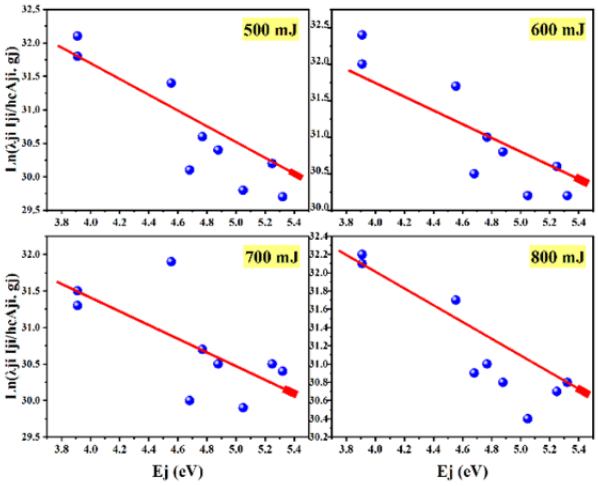

Figure 8. Boltzmann Plot for Various Laser Energy (500-800) mJ Values for a Copper Plate (Cu) Target in Laser-Induced Plasma

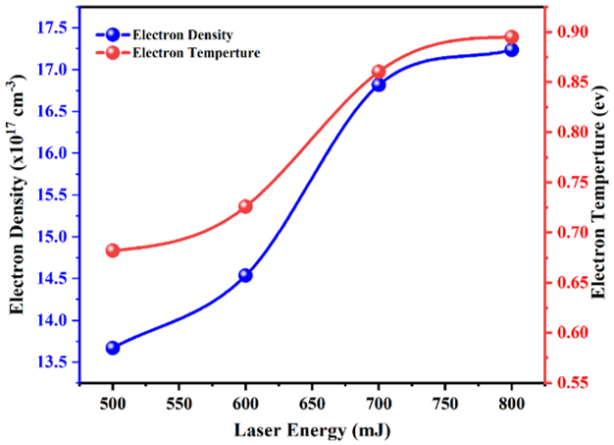

Figure 9. Relation of Electron Temperature (T_e) and Electron Density (n_e) with Increased Laser Energy (500-800) mJ for Copper Metal in Laser-Induced Plasma

When the laser bombardment begins, the generated ions and neutral particles will have a temperature near the surrounding temperature due to a progressive increase in energy from 500 mJ to a maximum of 800 mJ. However, the temperature of electrons rises significantly faster than that of neutral particles. Thus, the temperature of the electrons governs the extent of ionization in the created plasma (Onishi et al., 2021; Yaseen, 2016). This is especially significant since plasma ionization is controlled by electron temperature, which is related to ionization energy (Fikry et al., 2020a; Garcimuno et al., 2013). The results obtained indicated a perfect agreement between the electron temperature and the electron density with the gradual increase in the laser energy values during diagnosis, as the electron temperature values were 0.6820 eV at the laser energy 500 mJ until it reached 0.8949 eV at the energy 800 mJ, and this indicates a gradual rise in the measured electron temperature values, in addition, the measured electrode density values ranged from $(13.667\text{-}17.235)\times10^{17}$ cm^{-3}, where the results showed a direct proportion between the laser energy falling on the copper metal with the increase in the electron density values as shown in Figure 9 below.

According to the findings, the density and temperature of electrons increased proportionally with the increase in laser energy (500-800) mJ. Due to the significant effect of the increase in laser peak energy, both the intensity of the spectral lines and the target's mass ablation rate increased (Wu et al., 2021). By exposing the plasma to laser light for a longer duration, more ablation is produced, which increases the number of excited atoms and, consequently, the peak intensity values of the spectral lines of the plasma emission, as depicted in the pervious figure.

4. CONCLUSION

The results of this investigation, which involved detecting and analyzing copper plasma parameters, revealed a notable disparity between plasma electron temperature (T_e) and electron number density (n_e) as laser energy increased (500-800) mJ for pulses laser (10-30 pulses). The effect of the increased energy of the laser appears during the spectroscopic diagnosis and the process of metal bombardment shows three diameters or circles that can be described as the shape of a crater, the inner circle is close to brown and subjected to the strongest heating by the laser. Furthermore, the spectrum was recorded in the range of wavelengths from 200 nm to 650 nm, and there were numerous emission lines, including Cu(I), which were observed and began from weak intensity 311.83 nm and 324.58, 346.62, 360.20 nm to the most vigorous intensity 521.32 nm, as well as five ionic emission lines Cu(II), which started from weak line 212.54, 219.60, 237.82 nm, 261.97 to the strong

line at 529.42 nm of the energies (500-800) mJ. As a consequence of this research, the temperature and number density of electrons ranged from 0.6820 eV at 500 mJ and 0.8949 eV at 800 mJ, and (13.667-17.235)×10^{17} cm^{-3}, respectively, for the different laser energies.

5. ACKNOWLEDGMENT

I would like to express gratitude and grateful thanks and deeply extend thanks to the plasma laboratory in physics department-college of sciences/Baghdad University. And finally, I offer gratitude to everyone who gave me the inspiration to continue the thorough knowledge path.

REFERENCES

Ahmed, A. F. and A. A. Yousef (2021). Spectroscopic Analysis of DC-Nitrogen Plasma Produced using Copper Electrodes. *Iraqi Journal of Science*; 3560–3569

Akatsuka, H. (2019). Optical Emission Spectroscopic (OES) Analysis for Diagnostics of Electron Density and Temperature in Non-Equilibrium Argon Plasma Based on Collisional-Radiative Model. *Advances in Physics: X*, **4**(1); 1592707

Akhtar, M., A. Jabbar, N. Ahmed, S. Mahmood, Z. Umar, R. Ahmed, and M. Baig (2019). Analysis of Lead and Copper in Soil Samples by Laser-Induced Breakdown Spectroscopy Under External Magnetic Field. *Applied Physics B*, **125**(6); 1–11

Alberti, A., A. Munafò, M. Koll, M. Nishihara, C. Pantano, J. B. Freund, G. S. Elliott, and M. Panesi (2019). Laser-Induced Non-Equilibrium Plasma Kernel Dynamics. *Journal of Physics D: Applied Physics*, **53**(2); 025201

Benedikt, J., H. Kersten, and A. Piel (2021). Foundations of Measurement of Electrons, Ions and Species Fluxes Toward Surfaces in Low-Temperature Plasmas. *Plasma Sources Science and Technology*, **30**(3); 033001

Caneve, L., F. Colao, R. Fantoni, and V. Spizzichino (2006). Laser Ablation of Copper Based Alloys by Single and Double Pulse Laser Induced Breakdown Spectroscopy. *Applied Physics A*, **85**(2); 151–157

Chaudhary, K., S. Z. H. Rizvi, and J. Ali (2016). Laser-Induced Plasma and its Applications. *Plasma Science and Technology-Progress in Physical States and Chemical Reactions*; 259–291

Fernandes Andrade, D., E. R. Pereira-Filho, and D. Amarasiriwardena (2021). Current Trends in Laser-Induced Breakdown Spectroscopy: a Tutorial Review. *Applied Spectroscopy Reviews*, **56**(2); 98–114

Fikry, M., W. Tawfik, and M. Omar (2020a). Measurement of the Electron Temperature in a Metallic Copper using Ultrafast Laser-Induced Breakdown Spectroscopy. *Journal of Russian Laser Research*, **41**(5); 484–490

Fikry, M., W. Tawfik, and M. M. Omar (2020b). Investigation on the Effects of Laser Parameters on the Plasma Profile of Copper using Picosecond Laser Induced Plasma Spectroscopy. *Optical and Quantum Electronics*, **52**(5); 1–16

Garcimuno, M., D. D. Pace, and G. Bertuccelli (2013). Laser-Induced Breakdown Spectroscopy for Quantitative Analysis of Copper in Algae. *Optics & Laser Technology*, **47**; 26–30

Haberberger, D., A. Shvydky, V. Goncharov, D. Cao, J. Carroll-Nellenback, S. Hu, S. Ivancic, V. Karaseiv, J. Knauer, A. Maximov (2019). Plasma Density Measurements of the Inner Shell Release. *Physical Review Letters*, **123**(23); 235001

Kurniawan, G., F. Sa'adah, and A. Khumaeni (2018). Emission Characteristics of Copper using Laser-Induced Breakdown Spectroscopy at Low Pressure. *Journal of Physics: Conference Series*, **1025**; 012003

Maurya, G. S., A. Marín-Roldán, P. Veis, A. K. Pathak, and P. Sen (2020). A Review of the LIBS Analysis for the Plasma-Facing Components Diagnostics. *Journal of Nuclear Materials*, **541**; 152417

Onishi, H., F. Yamazaki, Y. Hakozaki, M. Takemura, A. Nezu, and H. Akatsuka (2021). Measurement of Electron Temperature and Density of Atmospheric-Pressure Non-Equilibrium Argon Plasma Examined with Optical Emission Spectroscopy. *Japanese Journal of Applied Physics*, **60**(2); 026002

Pathak, A. K., R. Kumar, V. K. Singh, R. Agrawal, S. Rai, and A. K. Rai (2012). Assessment of LIBS for Spectrochemical Analysis: a Review. *Applied Spectroscopy Reviews*, **47**(1); 14–40

Radziemski, L. J. (2020). *Lasers-Induced Plasmas and Applications*. CRC Press

Safeen, A., W. Shah, R. Khan, A. Shakeel, Y. Iqbal, G. Asghar, R. Khan, G. Khan, K. Safeen, and W. Shah (2019). Measurement of Plasma Parameters for Copper using Laser Induced Breakdown Spectroscopy. *Digest Journal of Nanomaterials and Biostructures*, **14**(1); 29–35

Shah, S. K. H., J. Iqbal, P. Ahmad, M. U. Khandaker, S. Haq, and M. Naeem (2020). Laser Induced Breakdown Spectroscopy Methods and Applications: a Comprehensive Review. *Radiation Physics and Chemistry*, **170**; 108666

Singh, J. P. and S. N. Thakur (2020). *Laser-Induced Breakdown Spectroscopy*. Elsevier

Wang, J. M., M. Panesi, and J. B. Freund (2021a). Thermal Effects Mediating the Flow Induced by Laser-Induced Optical Breakdown. *Physical Review Fluids*, **6**(6); 063403

Wang, Z., M. S. Afgan, W. Gu, Y. Song, Y. Wang, Z. Hou, W. Song, and Z. Li (2021b). Recent Advances in Laser-Induced Breakdown Spectroscopy Quantification: From Fundamental Understanding to Data Processing. *TrAC Trends in Analytical Chemistry*, **143**; 116385

Wu, F., J. Li, Y. Xian, X. Tan, and X. Lu (2021). Investigation on the Electron Density and Temperature in a Nanosecond Pulsed Helium Plasma Jet with Thomson Scattering. *Plasma Processes and Polymers*, **18**(8); 2100033

Yaseen, W. I. (2016). The Electron Temperature and the Electron Density Measurement by Optical Emission Spectroscopy in Laser Produced Aluminum Plasma in Air. *Iraqi Journal of Science*, **57**(2C); 1584–1590

Yuan, H., A. B. Gojani, I. B. Gornushkin, X. Wang, D. Liu, and M. Rong (2020). Dynamics of Laser-Induced Plasma Splitting. *Optics and Lasers in Engineering*, **124**; 105832

